Original Research

On the Synchronization of Transcranial Magnetic Stimulation and Functional Echo-Planar Imaging

Sven Bestmann, MSc,[1,2]* Jürgen Baudewig, PhD,[1] and Jens Frahm, PhD[1]

Purpose: To minimize artifacts in echo-planar imaging (EPI) of human brain function introduced by simultaneous transcranial magnetic stimulation (TMS).

Materials and Methods: Distortions due to TMS pulses (0.25 msec, 2.0 T) were studied at 2.0 T before and during EPI.

Results: Best results were obtained if both the EPI section orientation and the frequency-encoding gradient were parallel to the plane of the TMS coil. Under these conditions, a TMS pulse caused image distortions when preceding the EPI sequence by less than 100 msec. Recordings with a magnetic field gradient pick-up coil revealed transient magnetic fields after TMS, which are generated by eddy currents in the TMS coil. TMS during image acquisition completely spoiled all transverse magnetizations and induced disturbances ranging from image corruption to mild image blurring, depending on the affected low and high spatial frequencies. Simultaneous TMS and radio-frequency (RF) excitation gave rise to T1-dependent signal changes that lasted for several seconds and yielded pronounced false-positive activations during functional brain mapping.

Conclusion: To ensure reliable and robust combinations, TMS should be applied at least 100 msec before EPI while completely avoiding any pulses during imaging.

Key Words: magnetic resonance imaging; transcranial magnetic stimulation; human brain; BOLD; RF excitation; functional echo-planar imaging
J. Magn. Reson. Imaging 2003;17:309–316.

THE INTRODUCTION OF INTERLEAVED magnetic resonance imaging (MRI) and transcranial magnetic stimulation (TMS) has given the prospect of combining both methods for investigations of human brain function (1–7). Apart from providing access to the physiologic processes underlying the application of short pulses (0.25 msec) of intense magnetic field strength (2.0 T) to brain tissue, e.g., in terms of blood oxygenation level dependent (BOLD) MRI responses, the approach is expected to contribute new insights into the functional connectivity of the human brain, its "functional" plasticity using the concept of virtual lesions (8), and TMS-inducable neuronal plasticity.

Whereas most MRI studies hitherto focused on single TMS pulses (1,5) or low-frequency TMS at 1 Hz (3,4,6), applications in cognitive neuroscience often involve repetitive TMS at higher frequencies. Preliminary investigations of the effect of TMS at 10 Hz on the primary motor cortex (M1) indicated that the occurrence of a BOLD response after TMS requires the afferent feedback of an actual motor performance elicited only by TMS intensities above the active motor threshold (7). In contrast, sub-threshold TMS below the active motor threshold, which is known to act mainly at the intracortical circuitry (9), did not evoke BOLD responses underneath the TMS coil.

Despite the increasing interest in combined MRI-TMS studies, there is only limited information about the static and dynamic artifacts related to the TMS coil and magnetic pulse applications, respectively (2). In fact, the mere presence of a TMS coil may lead to image artifacts when using MRI sequences (such as EPI) that are susceptible to magnetic field inhomogeneities. Recently, corresponding signal losses and geometric distortions were shown to depend on the orientation and distance of the imaging section studied with respect to the TMS coil (10). While disturbances due to sparse TMS pulses could be minimized by sufficiently large waiting periods before imaging (4,6), TMS applications with higher stimulation frequencies still require a more detailed description of potential pitfalls. Therefore, the aim of the present work was to provide a comprehensive analysis of TMS-related EPI artifacts, and to develop a strategy for synchronizing high-frequency TMS with serial multi-slice EPI as commonly applied for mapping human brain function.

MATERIALS AND METHODS

Studies of healthy volunteers were approved by the local ethics committee according to the standards of the Declaration of Helsinki. All subjects gave informed written consent before all examinations.

[1]Biomedizinische NMR Forschungs GmbH, Max-Planck-Institut für biophysikalische Chemie, Göttingen, Germany.
[2]Sobell Department of Motor Neuroscience and Movement Disorders, Institute of Neurology, University College of London, London, UK.
Contract grant sponsor: DFG; Contract grant number: GK-GRK 632/1-00.
*Address reprint requests to: S.B., Biomedizinische NMR Forschungs GmbH, Max-Planck-Institut für biophysikalische Chemie, Am Fassberg 11, 37077 Göttingen, Germany. E-mail: sbestma@gwdg.de
Received July 22, 2002; Accepted October 30, 2002.
DOI 10.1002/jmri.10260
Published online in Wiley InterScience (www.interscience.wiley.com).

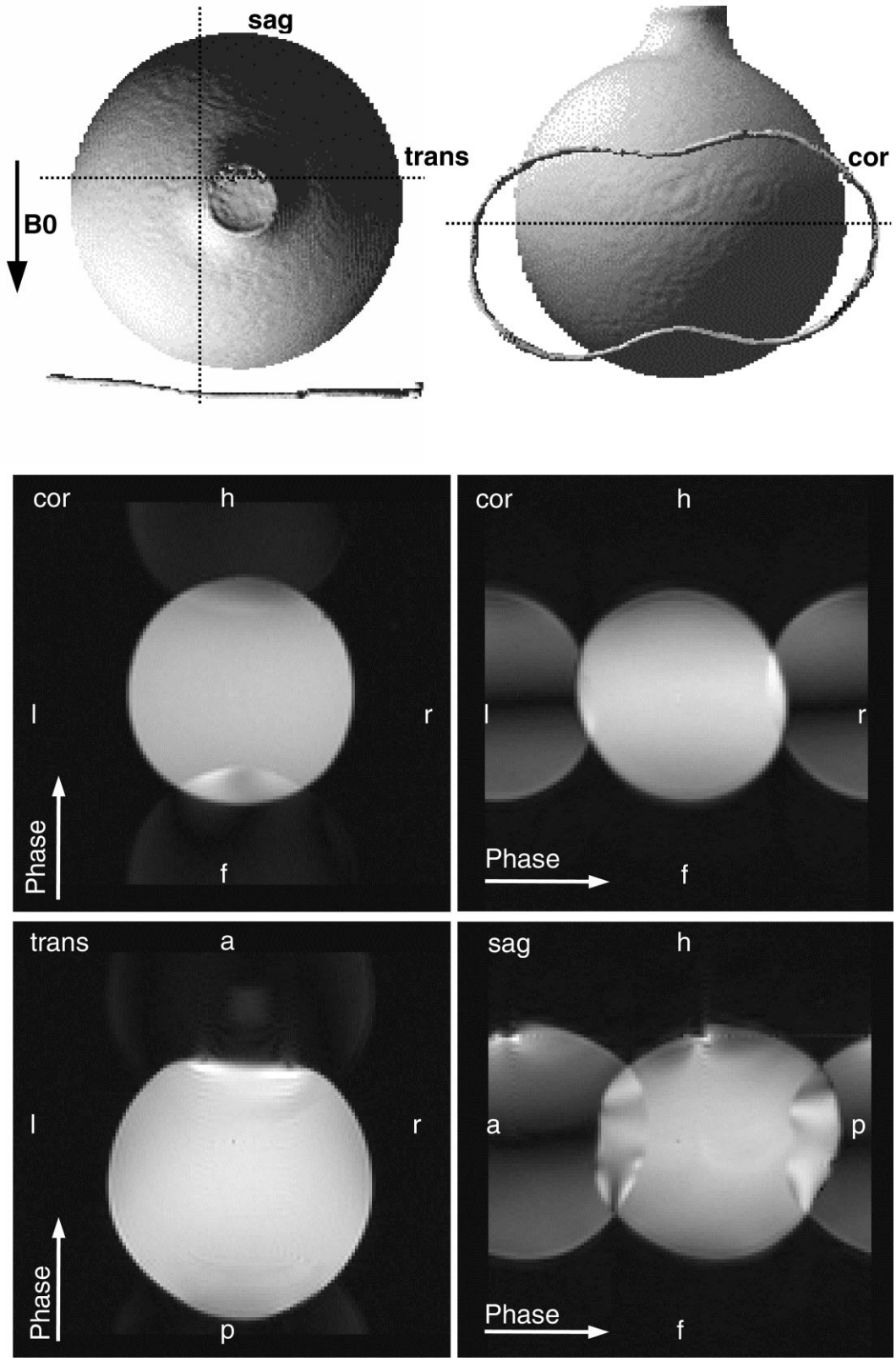

Figure 1. Top: Top and frontal view of a spherical water phantom (surface reconstruction, 3D FLASH) with a transverse orientation of the figure-eight TMS coil (long axis 190 mm) highlighted by a water-filled plastic hose (arrow: static magnetic field; broken lines: EPI sections). With this coil configuration, the static magnetic field and the TMS-induced magnetic field oppose each other. **Middle:** In coronal sections, a switch of the frequency- and phase-encoding gradient largely reduces ghosting artifacts. **Bottom:** Transverse section at 6-cm distance from the TMS coil and sagittal section (a = anterior, cor = coronal, f = foot, h = head, l = left, r = right, sag = sagittal, trans = transverse, phase = phase-encoding gradient axis, p = posterior).

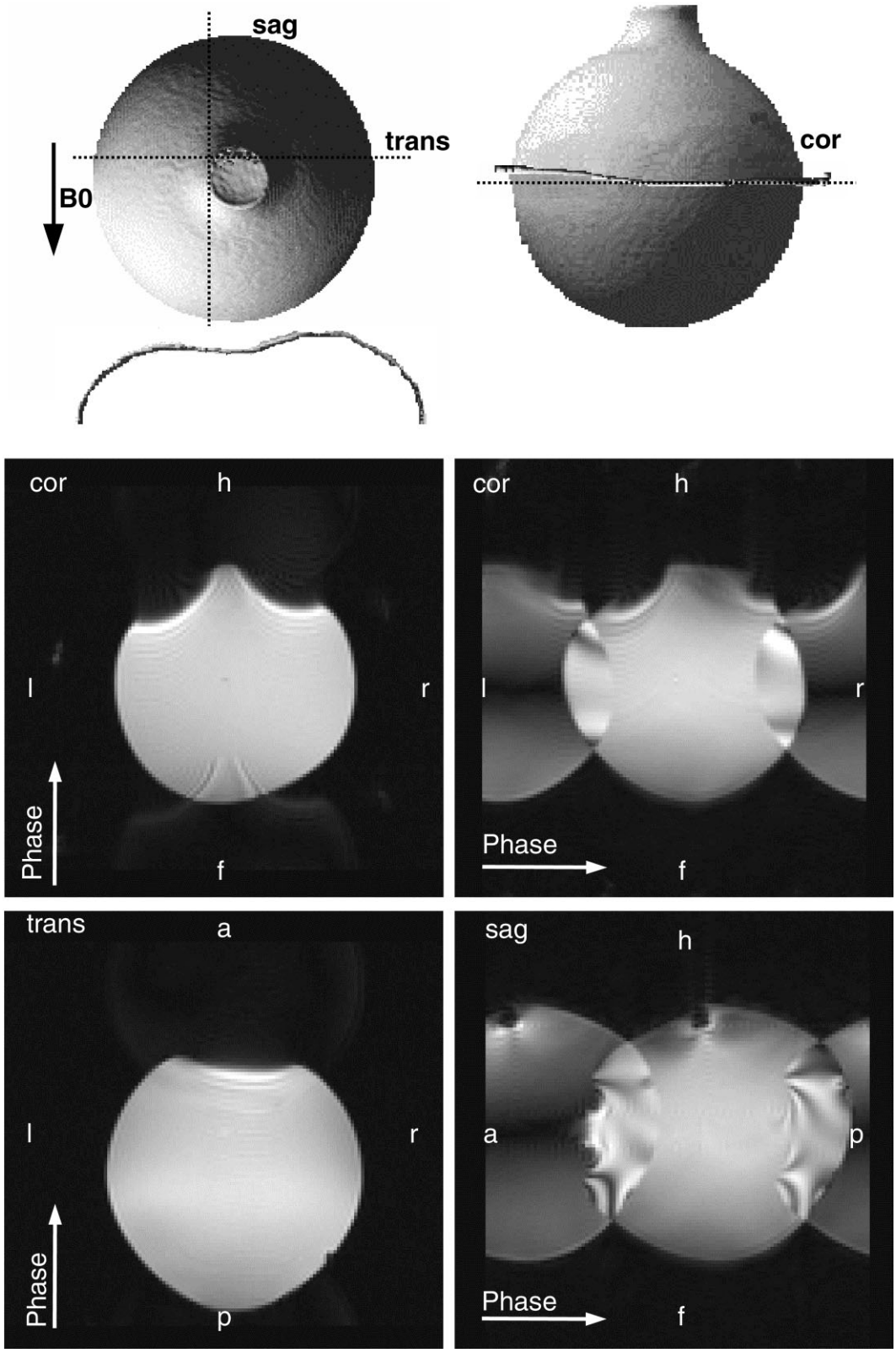

Figure 2. Top: Top and frontal view of a spherical water phantom with a coronal orientation of the TMS coil. At this orientation, the induced magnetic field runs perpendicular to the static magnetic field. Coronal section (**middle**) as well as transverse section (**bottom**) at 6-cm distance from the TMS coil and sagittal section. Abbreviations as in Figure 1.

Transcranial Magnetic Stimulation

TMS with biphasic pulses was performed using a MagStim Rapid stimulator and a figure-of-eight coil with a long axis of 190 mm and a diameter of 100 mm (The Magstim Company, Wales, UK). The coil was specially designed for MRI and did not contain any ferromagnetic materials. A custom-made, adjustable plastic holder was attached to the MRI headcoil, which allowed positioning and fixation of the TMS coil with several degrees of freedom. A water-filled plastic hose was attached along the outer coil surface to identify its position by MRI. The coil was connected to the TMS stimulator outside the radio frequency (RF)-shielded cabin through an RF filter tube, using a cable of 8-m length. For precise synchronization of TMS pulses and MRI data acquisition, a 5-V TTL pulse was derived from the EPI sequence at the time of each RF excitation pulse and fed into the printer port of a personal computer with a DOS operating system. Accurate TMS triggering was accomplished by a C program developed in-house. No modifications of either the TMS stimulator or MRI hardware were required.

Echo-Planar Imaging

All studies were conducted at 2.0 Tesla (Siemens Magnetom Vision, Erlangen, Germany) using the standard imaging headcoil. Phantom studies involved a water-filled spherical glass container. Additional experiments were performed with use of a 15% Agar solution to exclude vibration-related fluid movements as a putative source of MRI signal alteration. Structural MRI was based on 3D FLASH (TR/TE = 15/4 msec, flip angle 20°, 1 × 1 × 2 mm^3 resolution) covering the whole phantom or head, while T2*-weighted acquisitions were accomplished with use of single-shot, blipped gradient-echo EPI (TR = 2000 msec, mean TE = 54 msec, symmetric coverage of k-space, echo train length 113 msec, flip angle 70°) at 2 × 2 ×4 mm^3 resolution, as commonly applied for functional mapping in this laboratory.

All phantom studies were analyzed with in-house software. Signal intensities of each image were calculated without spatial or temporal filtering in a region-of-interest covering the image center. Determination of the coil position was achieved by 3D surface reconstruction of T1-weighted images using BRAIN VOYAGER 3.0 (Brain Innovation BV, The Netherlands).

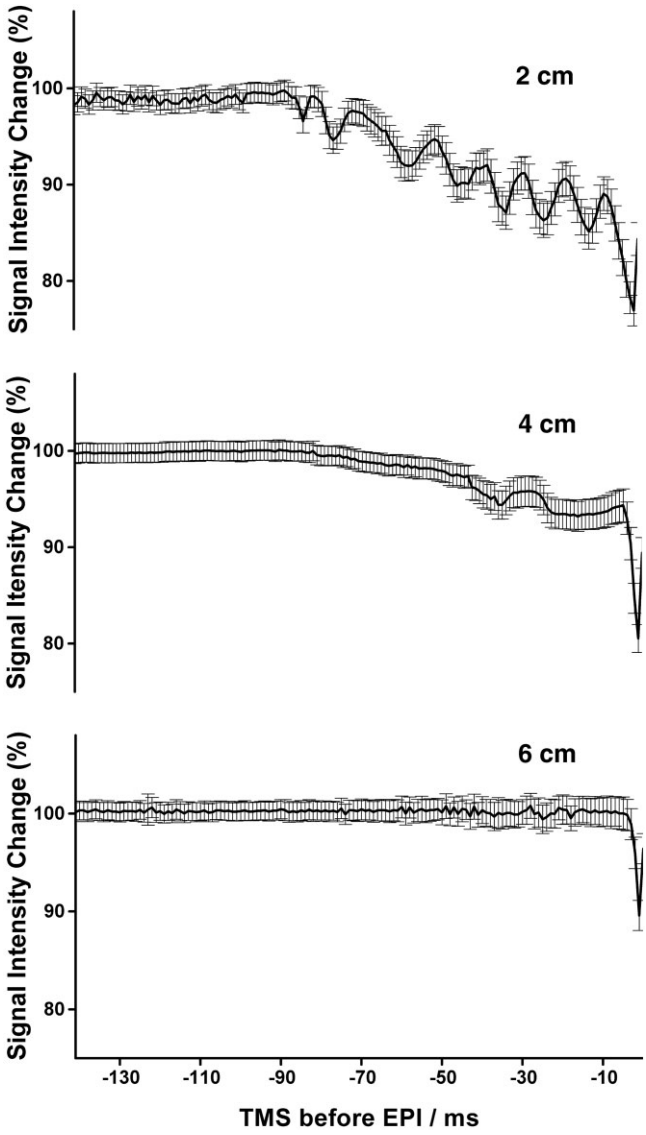

Figure 3. EPI signal intensity changes (mean ± SD) from a central region-of-interest of transverse sections through the phantom shown in Fig. 1 at 2 cm, 4 cm, and 6 cm distance from the TMS coil as a function of time (1-msec steps) between a single TMS pulse (100% stimulator output) and the EPI RF excitation pulse. For waiting periods of less than about 100 msec, the data reveal signal fluctuations of up to 20% for the closest section; these decrease with increasing distance.

Combined TMS and EPI

Extending a previous study (10), the influence of a TMS coil on the quality of gradient-echo EPI was systematically tested for different orientations of the coil (transversal, coronal) and imaging gradients (slice selection, phase encoding, frequency encoding), excluding only those EPI combinations that are beyond human safety recommendations. Subsequently, the dynamic effects associated with the application of TMS pulses were investigated as a function of time before and during EPI. The study comprised four different parts:

1. TMS before EPI: because previous work suggested that images may be affected even 100 msec after a TMS pulse (2), the effect of a single TMS pulse on a single EPI section oriented parallel to the TMS coil was studied as a function of time (1-msec steps) for various coil-slice distances (2 cm, 4 cm, and 6 cm) and TMS pulse intensities (50% and 100% of stimulator output). In addition, to assess induced eddy currents as a potential source of image degradation (2), a magnetic resonance gradient pick-up coil recorded field fluctuations after TMS.
2. TMS during data acquisition: high-frequency TMS in conjunction with multi-slice EPI aggravate the difficulty of embedding repetitive TMS pulses within serial EPI acquisitions. Although it has been reported that reasonable image quality may

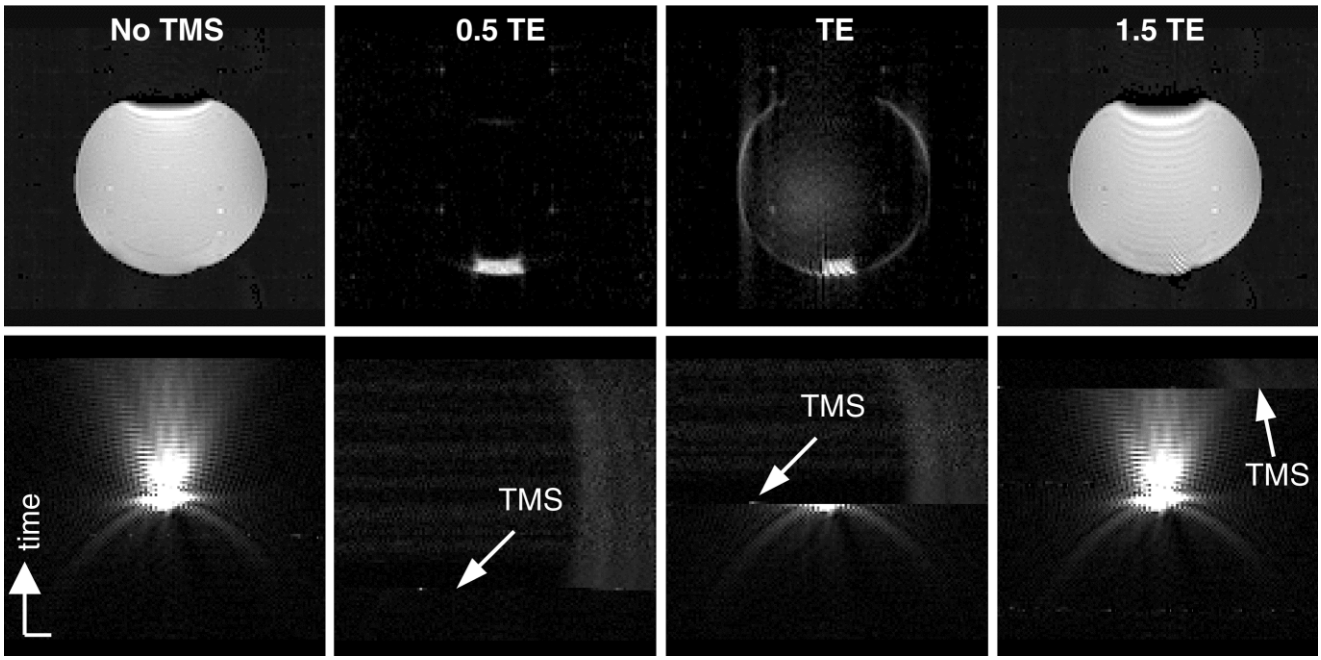

Figure 4. Effects of a single TMS pulse on EPI (**top**) and corresponding raw data sets (**bottom**) when applied at different times during data acquisition (mean TE = 54 msec, echo train length 113 msec) for a transverse section at 6-cm distance from the TMS coil (other parameters as in Fig. 3). Whereas TMS pulses cause dramatic signal losses during the acquisition of the first half of k-space, reasonable images may be obtained at later periods after scanning about 3/4 of k-space (1.5 TE).

be achieved with TMS pulses applied shortly after the mean TE (2), a more comprehensive examination addressed the effects of a single TMS pulse at variable times (1-msec steps) during data readout, i.e., as a function of the affected high and low spatial frequencies, for different coil-slice distances (2 cm, 4 cm, and 6 cm).

3. TMS during RF excitation: although a disturbance of the slice-selective RF excitation by a simultaneous TMS pulse will likely be expected, its translation into longitudinal magnetization may cause persistent alterations extending the acquisition of the directly affected image. Therefore, a single TMS pulse was applied 4 msec after the onset of the RF excitation pulse (9.6 msec, sinc profile) of an EPI sequence, and changes in EPI signal intensity of subsequent images were examined as a function of time for various repetition times and flip angles.
4. TMS during functional brain mapping: to demonstrate the confounding effects of TMS on functional EPI of human brain activation (TR = 2000 msec, eight sections), a single TMS pulse was applied to the left-hemispheric M1 of a right-handed male subject (age 26 years, no neurologic or psychiatric predisposition) during functional mapping of BOLD responses to a sequential finger-to-thumb opposition task of the dominant hand (visually cued tapping of individual fingers against the thumb at 2 Hz). The paradigm consisted of eight cycles of 10-second tapping epochs followed by 20-second rest epochs. The position of the TMS coil atop M1 was determined inside the scanner, but without imaging, by applying suprathreshold TMS pulses with a posterior-anterior current orientation. During functional EPI, a single subthreshold TMS pulse (39% stimulator output, active motor threshold 45%) was synchronized to coincide with a single RF pulse exciting only one of the sections at the start of each finger-tapping epoch. The validity of the mapping procedure was tested by repeating the task without TMS.

Task-related EPI signal changes were identified by cross-correlation with a boxcar reference function matching the finger-tapping protocol with a shift by one image (2 seconds) to account for hemodynamic delays. Quantitative activation maps were obtained by automated user-independent statistical procedures (in-house software), rescaling the histogram of all correlation coefficients per map as percentile ranks of the underlying noise distribution (11). In an iterative procedure, pixels above the 99.99% percentile rank are identified as activated (corresponding to a type-one error probability of $P < 0.0001$) and, subsequently, directly neighboring pixels exceeding a 95% percentile rank are added (corresponding to an type-one error probability of $P < 0.05$).

RESULTS

Figure 1 summarizes the key findings for EPI effects introduced by the presence of a TMS coil. For the coil-phantom arrangement chosen here, strong artifacts were obtained whenever the frequency-encoding gradient was pointing through the plane of the TMS coil. These distortions occurred regardless of whether the image section was cutting through the TMS coil plane

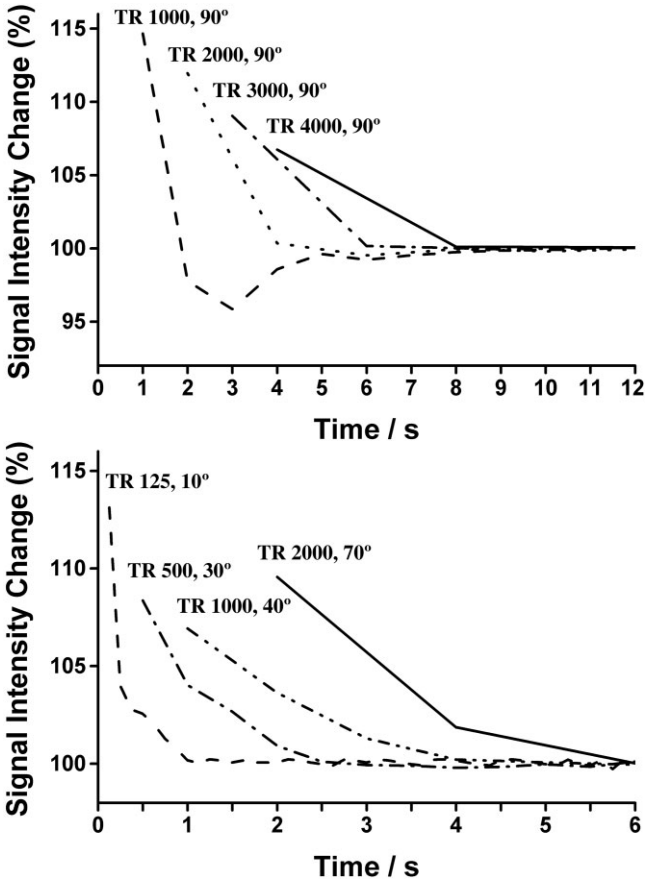

Figure 5. EPI signal intensity changes in successive acquisitions after application of a single TMS pulse during RF excitation of the first image (omitted) as a function of time for various TR repetition times and flip angles (transverse section at 6-cm distance from the TMS coil; other parameters as in Fig. 3). Depending on the degree of T1 saturation, the data reveal long-lasting signal fluctuations due to a disturbance of the steady-state longitudinal magnetization.

or not. For coronal sections, a switch of the frequency- and phase-encoding gradient largely reduced the ghosting artifacts. Similarly, transverse sections at some distance apart from the coil, and with phase-encoding gradients in a posterior-anterior direction, revealed only negligible distortions. On the other hand, and in line with previous observations (10), a distance of only 2 cm was insufficient to avoid severe artifacts (not shown). Although similar results were observed for a coronal orientation of the TMS coil as shown in Figure 2, direct susceptibility artifacts were significantly more pronounced. In general, best results were obtained if both the section orientation and the frequency-encoding gradient were parallel to the plane of the TMS coil.

Under such optimized conditions, Figure 3 shows signal intensity changes from transverse sections of the same phantom as in Figure 1 that are induced by the application of a single TMS pulse at variable times before the EPI sequence. The data reveal signal alterations for waiting periods after TMS of less than about 100 msec, which decrease in amplitude with increasing section distance from the TMS coil. It should be noted that such intensity variations are difficult to detect by inspection of individual images because visible image distortions only occurred for TMS pulses at 30–50 msec or less before the RF pulse.

Complementary to these imaging results, a magnetic field gradient pick-up coil 2 cm underneath the TMS coil detected transient magnetic fields that lasted for up to 35 msec. These fields were attenuated when the distance of the pick-up coil from the TMS coil was increased to 4 cm or 6 cm, and enhanced for TMS coil orientations, which resulted in magnetic fields opposing the static field of the MRI system and thus larger torques. In general, both the EPI artifacts and transient magnetic fields decreased in amplitude when the TMS intensity was reduced from 100% to 50% of maximum stimulator output.

The degrading effect of a TMS pulse during EPI is demonstrated in Figure 4. Almost independent of the distance from the coil, the application of a TMS pulse during the first half of data acquisition, i.e., before the acquisition of the low spatial frequencies, causes a complete loss of signal. As evident from the raw data sets, the physical reason is an effective spoiling of all transverse magnetizations, i.e., gradient echoes, after the TMS pulse. With increasing waiting periods after the onset of data acquisition, the resulting image quality gradually recovers to that obtainable without a TMS pulse. This holds true particularly for TMS pulses applied after recording about 3/4 of k-space at echo times greater than the mean TE. Although such TMS pulses still eliminate all residual gradient echoes, the images present with only minor high-frequency distortions.

The direct interference of a TMS pulse with the RF excitation process not only corrupts the affected image, but also increases the signal intensity in subsequent acquisitions. As shown in Figure 5, the duration and magnitude of respective EPI signal changes in successive images are dependent on the repetition time and flip angle, i.e., the degree of T1 saturation imposed onto the steady-state magnetization. They may reach amplitudes of up to 15% and last for up to 8 seconds for pronounced T1 saturation, e.g. TR = 1000 msec and 90°, and only about 1 second for spin-density weighted EPI, e.g., TR = 125 msec and 10°. Again, it should be emphasized that these effects are not necessarily visible as geometric distortions in individual images.

The persistent signal changes associated with TMS pulses synchronized to the beginning of an EPI sequence, i.e., close to RF excitation, pose a major problem for combinations with functional brain mapping. An example is shown in Figure 6, comparing activation maps obtained with and without TMS. In the absence of TMS, the finger-to-thumb opposition task activates M1 and the supplementary motor area (SMA) in the sections shown. A single TMS pulse applied to the RF pulse of the middle section in Figure 6 at the start of each finger-tapping epoch results in marked false-positive activations even when the single corrupted image is eliminated from the analysis. Pertinent effects mainly occur at contrast borders with CSF (long T1). The fact that spatially, but not temporally, adjacent sections reveal similar false-positive activations supports the notion that the underlying mechanism is not due to the TMS pulse itself, but represents a longer-lasting distur-

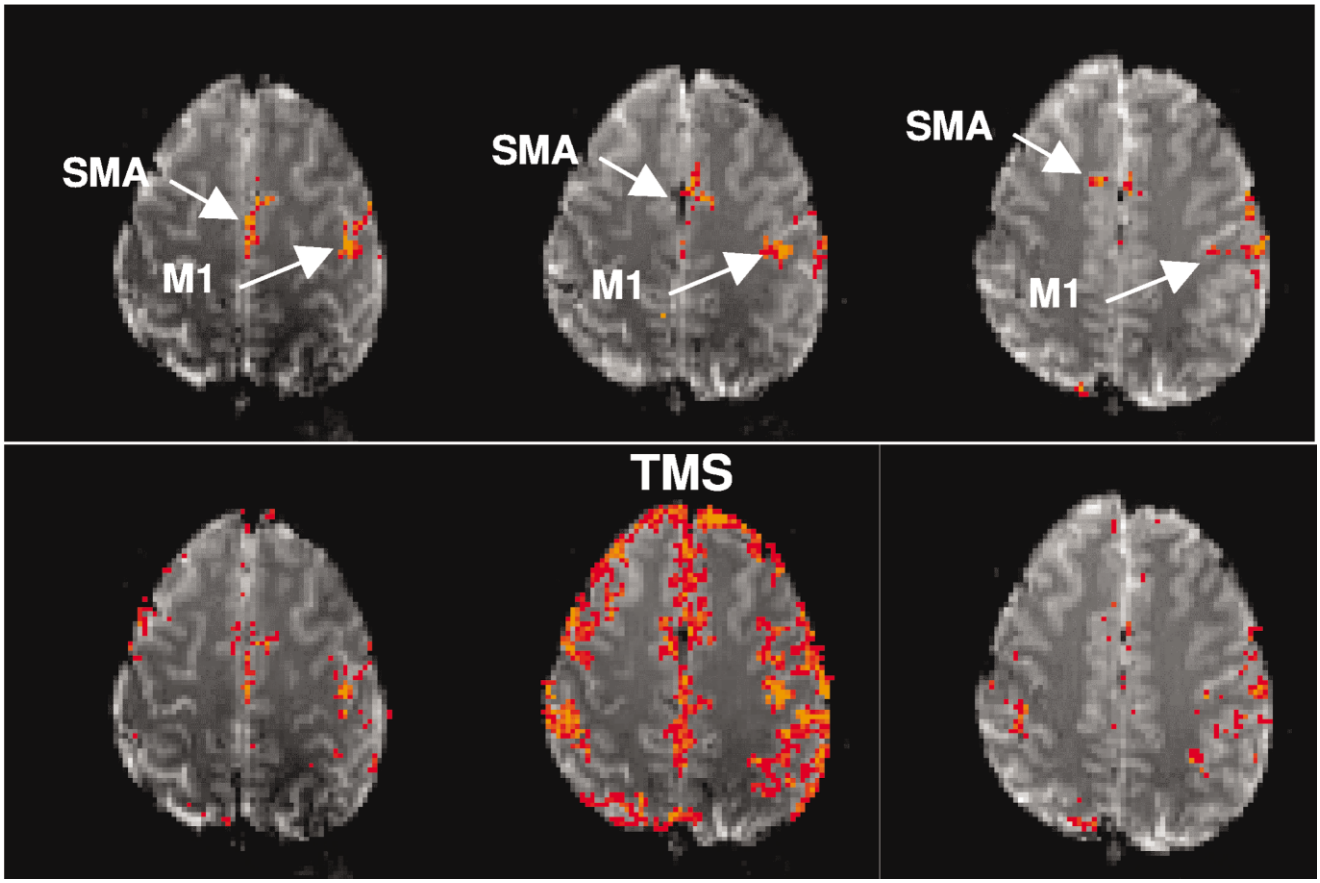

Figure 6. Functional activation maps (3/8 neighboring sections) for a sequential finger-to-thumb opposition task obtained without (**top**) and with (**bottom**) TMS. A single TMS pulse during RF excitation of the first set of multi-slice images in each finger-tapping epoch (affecting the **middle** section only) causes a task-related perturbation of the steady-state longitudinal magnetization, which translates into false-positive activations.

bance of the steady-state magnetization concurrent with task performance.

DISCUSSION

Extending the work of Baudewig and colleagues (10), combinations of TMS and EPI benefit from a parallel arrangement of the TMS coil plane with both the MRI section orientation and the frequency-encoding gradient. Because such ideal geometric conditions are seldom applicable for successful stimulation of the cortex, the use of oblique TMS coil orientations is expected to enhance image distortions. In general, such considerations together with EPI safety restraints and the need for multi-slice volume coverage limit the degree of freedom for a placement of the TMS coil. Whether technical improvements such as better coil designs, more tolerable imaging sequences, or even faster imaging techniques will enhance the flexibility of combined TMS and MRI studies remains to be seen.

The basic problem of TMS and MRI is that the TMS pulse itself represents an extremely efficient spoiler gradient that eliminates all transverse magnetizations. In addition, a TMS pulse generates magnetic field fluctuations for up to 100 msec that originate from eddy currents in the TMS coil. The underlying mechanism is based on the torque such a coil experiences in response to a pulse discharge. It generates a rapid mechanical vibration of the coil easily noted as a "click" sound. The torque and therefore also the loudness of the sound increase in the static magnetic field of the MRI scanner, and in particular for orientations opposing the MRI field. The vibrations lead to currents in the TMS coil by electromagnetic induction which, in turn, cause weak magnetic fields perpendicular to the coil plane. Without sufficiently long waiting periods, these transient fields modulate the imaging gradients of subsequent EPI sequences.

The aforementioned explanation is in contrast to a previous suggestion that TMS-induced image degradations are due to eddy currents induced in the conducting structures of the MRI system (2). In fact, the present understanding is strongly supported by the observation that both the strength of the transient magnetic fields measured directly by a pick-up coil and the image artifacts detected in subsequent EPI acquisitions decreased with increasing distance from the TMS coil. On the other hand, eddy currents in the scanner elements should affect the entire volume within the magnet bore, which is in contrast to the experimental behavior. It

may be argued that the directly detected magnetic field fluctuations lasted for only 35 msec and therefore cannot account for all of the EPI impairments. However, this apparent conflict has to be ascribed to the limited sensitivity of the pick-up coil in comparison with the susceptibility of imaging gradients to even weak magnetic gradient fields.

Depending on the temporal relationship between TMS and EPI, either the TMS pulse itself or its accompanying magnetic field fluctuations will have different consequences. First, while waiting periods after TMS and before EPI of 50–100 msec may alter EPI signal intensities, periods of less than 30–50 msec cause geometric distortions. Second, during EPI, TMS pulses operate as efficient spoiler gradients that completely dephase transverse magnetizations and thus eliminate the residual echo train. Depending on which parts of the k-space acquisition are affected, the artifacts in Fourier space range from complete image corruption to complex modulations of the point-spread-function and the presence of mild blurring. Third, when affecting RF excitation, TMS pulses alter the steady-state longitudinal magnetization with severe consequences for serial imaging as used in functional brain mapping.

CONCLUSION

In conclusion, in order to minimize image artifacts, any direct interference of TMS and EPI should be avoided. Alternatively, the experimental design must allow for an unambiguous identification and elimination of perturbed images, as inappropriate timing of TMS pulses may not only degrade the quality of individual images but also cause dynamic signal fluctuations in serial acquisitions. Provided that proper synchronization ensures a sufficient temporal decoupling of about 100 msec, interleaved high-frequency TMS and multi-slice EPI will further develop into a useful tool for clinical and cognitive neuroscience.

ACKNOWLEDGMENTS

The authors are grateful to Anthony Thomas for providing the TMS coil, Drs. Walter Paulus and Peter Dechent for scientific guidance, and Peter Wenig, Lutz Präkelt, and Jörg Bertram for technical support. SB was supported by a grant from the DFG (GK-GRK 632/1-00).

REFERENCES

1. Bohning DE, Shastri A, Nahas Z, et al. Echoplanar BOLD fMRI of brain activation induced by concurrent transcranial magnetic stimulation. Invest Radiol 1998;33:336–340.
2. Shastri A, George MS, Bohning DE. Performance of a system for interleaving transcranial magnetic stimulation with steady-state magnetic resonance imaging. Electroencephalogr Clin Neurophysiol Suppl 1999;51:55–64.
3. Bohning DE, Shastri A, McConnell KA, et al. A combined TMS/fMRI study of intensity-dependent TMS over motor cortex. Biol Psychiatry 1999;45:385–394.
4. Bohning DE, Shastri A, McGavin L, et al. Motor cortex brain activity induced by 1-Hz transcranial magnetic stimulation is similar in location and level to that for volitional movement. Invest Radiol 2000;11:676–683.
5. Bohning DE, Shastri A, Wassermann EM, et al. BOLD-fMRI response to single-pulse transcranial magnetic stimulation (TMS). J Magn Reson Imaging 2000;11:569–574.
6. Nahas Z, Lomarev M, Roberts DR, et al. Unilateral left prefrontal transcranial magnetic stimulation (TMS) produces intensity-dependent bilateral effects as measured by interleaved BOLD fMRI. Biol Psychiatry 2001;50:712–720.
7. Baudewig J, Siebner HR, Bestmann S, et al. Functional MRI of cortical activations induced by transcranial magnetic stimulation (TMS). Neuroreport 2001;12:3543–3548.
8. Pascual-Leone A, Walsh V, Rothwell J. Transcranial magnetic stimulation in cognitive neuroscience - virtual lesion, chronometry, and functional connectivity. Curr Opin Neurobiol 2000;10:232–237.
9. Di Lazzaro V, Restuccia D, Oliviero A, et al. Magnetic transcranial stimulation at intensities below active motor threshold activates intracortical inhibitory circuits. Exp Brain Res 1998;119:265–268.
10. Baudewig J, Paulus W, Frahm J. Artifacts caused by transcranial magnetic stimulation coils and EEG electrodes in T2*-weighted echo-planar imaging. Magn Reson Imaging 2000;18:479–484.
11. Kleinschmidt A, Requardt M, Merboldt KD, Frahm J. On the use of temporal correlation coefficients for magnetic resonance mapping of functional brain activation. Individualized thresholds and spatial response delineation. Int J Imaging Syst Technol 1995;6:238–244.